Looking Down Through the Clouds – Optical Attenuation through Real-Time Clouds

Jarred Burley
Air Force Institute of Technology
Andrew Lazarewicz, Devin Dean, Nicholas Heath
Air Force Technical Applications Center

2017 Advanced Maui Optical and Space Surveillance Conference (AMOS)
Wailea Marriott, Maui, Hawaii
19-22 September 2017

Abstract

Detecting and identifying nuclear explosions in the atmosphere and on the surface of the Earth is critical for the Air Force Technical Applications Center (AFTAC) treaty monitoring mission. Optical signals, from surface or atmospheric nuclear explosions detected by satellite sensors, are attenuated by the atmosphere and clouds. Clouds present a particularly complex challenge as they cover up to seventy percent of the earth's surface. Moreover, their highly variable and diverse nature requires physics-based modeling. Determining the attenuation for each optical ray-path is uniquely dependent on the source geolocation, the specific optical transmission characteristics along that ray path, and sensor detection capabilities. This research details a collaborative AFTAC and AFIT effort to fuse worldwide weather data, from a variety of sources, to provide near-real-time profiles of atmospheric and cloud conditions and the resulting radiative transfer analysis for virtually any wavelength(s) of interest from source to satellite. AFIT has developed a means to model global clouds using the U.S. Air Force's World Wide Merged Cloud Analysis (WWMCA) cloud data in a new toolset that enables radiance calculations through clouds from UV to RF wavelengths.

1. Introduction

In 1947, President Eisenhower charged the Army Air Force with the mission to detect nuclear detonations (NUDET) anywhere on Earth. Today, the Air Force Technical Applications Center (AFTAC), located at Patrick AFB, FL, fulfills this request and is charged with nuclear treaty monitoring in all of Earth's geophysical environments (underground, in the ocean, on the surface, in the atmosphere and in space).

A specific AFTAC mission is to monitor nuclear detonations (NUDETS) on or near the Earth's surface, land or ocean, using optical sensors on orbit in space. A specific technical parameter of interest is the attenuation of optical signals, from the Earth's surface to a space-borne sensor, for its specific ray-path. That originating optical signal, with its own spectral and spatial characteristics, changes its characteristics as it travels through the Earth's atmosphere and clouds, and is then detected in space with an optical sensor with its own spectral characteristics. In AFTAC's case, the objective is to determine the characteristics of the originating optical signal from the measured optical signal by accounting for the physics of the entire, and specific, optical path.

The global static and climatic characteristics of the Earth's atmosphere have generally been established and studied with a variety of different models and tools. However, real-time or near-real-time effects of clouds along specific optical ray paths has been an elusive goal. The problem addressed in this paper is to develop methods that allow an analyst to determine the effects of local clouds for specific ray paths, in real-time. The answer can have broad applications across many missions and projects, but is particularly of interest to AFTAC for evaluating received optical data from orbiting sensors.

Clouds, weather, and aerosol conditions can significantly modify a signal of interest and their effects cannot be quickly modeled using global atmospheric and climatic models. Of particular interest is the ability to use the atmosphere, and specifically clouds, as a filter for geolocation via non-imaging detectors. To this end, a new Air

Copyright © 2017 Advanced Maui Optical and Space Surveillance Technologies Conference (AMOS) – www.amostech.com

Force Institute of Technology (AFIT) toolset is leveraged to demonstrate improved remote sensing analysis capability as applied to NUDET detection and analysis. The AFIT toolset provides a breakthrough improvement in analyzing Earth to space (or vice-versa) optical signals. The partnership of AFIT and AFTAC also demonstrates a breakthrough opportunity to advance AFIT's technology for operational use at AFTAC.

2. Atmospheric Characterization

Characterizing atmospheric conditions in near-real time presents a challenge because atmospheric processes are dynamic and constantly changing. Historically, meteorological conditions have been observed and recorded at numerous sites and locations. Vertical profiles have long been determined via balloon based sensors at multiple sites world-wide. Surface observations are typically plentiful, especially at airfields and other aviation related locations. Despite localized observations, it is common practice to define model atmospheres, such as the 1976 U.S. Standard atmosphere, that represent average or expected atmospheric conditions for use in modeling. These are particularly useful in evaluating model performance relative to other models as they provide a standardized initialization input; however, they fail to account for actual weather conditions. Climatological conditions provide a realistic estimate on bounds of conditions, but more accurate solutions can be obtained using Numerical Weather Prediction (NWP) data and real-time observations [1].

NWP data provide correlated, gap-filled, gridded, near-real-time depictions of atmospheric conditions throughout the vertical extent of the atmosphere as both analysis and forecast products. The sophistication of these weather prediction models has greatly improved with the advancement of computational capability. For this research, Global Forecast System (GFS) output obtained through the NOAA Operational Model Archive and Distribution System (NOMADS) was utilized due its availability and global coverage [2, 3]. While other models provide finer resolution and spatial coverage, the world-wide coverage of the GFS is essential to demonstrate potential operational impacts. Here, we use GFS output available on a 0.5 x 0.5 degree grid with 26 vertical layers. The top of the model is generally around 30-32 km depending on geographic location [3]. The model output is generated four times per day with 3-hour forecast time steps out to 240 hours and 12-hour time steps out to 384 hours. The parameters utilized in this research to build correlated atmospheric profiles include pressure, temperature, relative humidity, and surface altitude. Figure 1 shows an example of GFS data (temperature and dew point) used in this research.

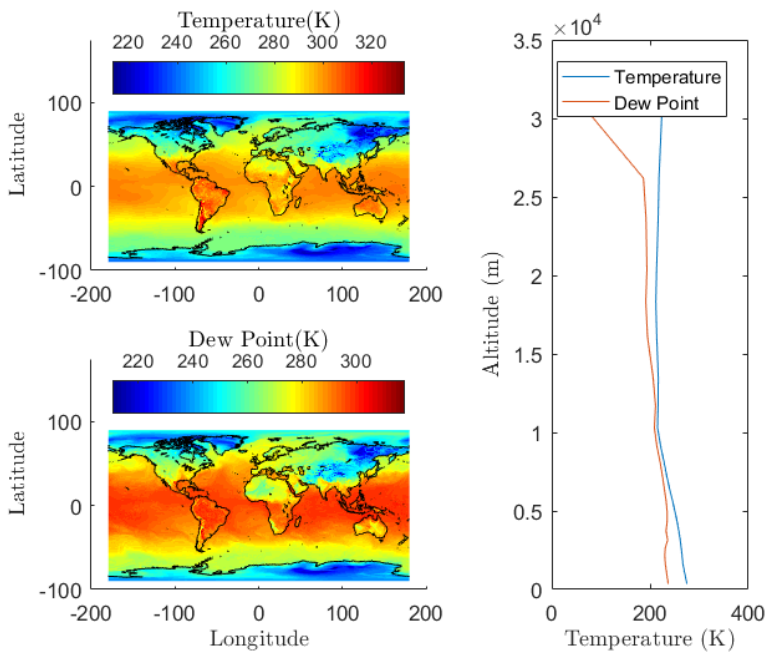

Fig. 1. Example GFS temperature and dew point profiles. The top left plot depicts worldwide temperatures on 14 Dec 2014 at 1800 UTC while the bottom left plot depicts the dew point for the same time period. The right plot shows the vertical profile for temperature and dew point at 40º latitude and -84º longitude [4].

Copyright © 2017 Advanced Maui Optical and Space Surveillance Technologies Conference (AMOS) – www.amostech.com

Clouds were incorporated into the atmospheric profiles by leveraging data from the World Wide Merged Cloud Analysis (WWMCA) product from the U.S. Air Force's 557th Weather Wing. WWMCA merges both satellite and ground based cloud observations into a world-wide gridded product that is produced hourly, providing a snapshot of the atmospheric cloud state. Distributed on a 0.25 x 0.25 degree grid and modified with a forecaster in the loop for quality control, WWMCA produces several valuable cloud parameters. The ones used in this research include cloud top height, cloud bottom height, total cloud cover, cloud type, water path, ice water percentage, cloud effective particle diameter, and cloud optical depth [5].

Integration of the cloud parameters into a vertical profile is accomplished by describing the effective cloud droplet size with a modified gamma distribution of the form

$$\frac{dN}{dr} = Nar^{(1-3\nu_{eff})/\nu_{eff}} \exp\left[-\frac{r}{r_{eff}\nu_{eff}}\right]$$

where ν_{eff} is the effective variance of the distribution and $N \times a$ is the normalization coefficient. By assuming an effective variance, as done for operational satellite collections [6], the size distribution can be described in terms of cloud effective radius. Applying Mie theory via the Wiscombe Mie scattering module incorporated in LEEDR, absorption and scattering efficiencies and phase functions are obtained [7]. Cloud boundaries are determined from the WWMCA outputs and the cloud is considered uniform between the top and bottom. These meteorological and cloud properties are essential for building vertical profiles used for simulating radiative transfer effects.

3. Radiative Transfer Modeling

The Laser Environmental Effects Definition and Reference (LEEDR) is a verified and validated atmospheric characterization package designed to define correlated atmospheric profiles of temperature, pressure, water vapor content, optical turbulence, and atmospheric particulates and hydrometeors as they relate to line-by-line and spectral band solutions for layer extinction coefficient magnitude for any wavelengths from 200 nm to 8.6 m [8]. The key difference between LEEDR and other radiative transfer software packages is the physically realizable atmospheric definitions that enables accurate characterization of line-by-line and spectral band effects. As a default, LEEDR relies on correlated atmospheric databases from worldwide climatological data to describe the temporally and spatially varying aerosol and hydrometeor profiles used in its radiative transfer calculations. LEEDR also uses unique boundary layer definitions and descriptions to capture the adiabatic nature of the boundary layer and the subsequent vertical variability or aerosol size distributions. The default climatological data covers 30+ years for 573 land sites and 1 x 1 degree ocean areas [9].

In addition to the climatological data described above, LEEDR can also be coupled with NWP data to produce outputs of absorption, scattering, and total extinction layer coefficients that are used to more realistically describe the radiative transfer properties of the atmosphere. When compiled over a geographic volume and assembled together, this provides visually stunning and physically realistic 4D visible-spectrum images, known as Weather Cubes, which accurately translate propagation and atmospheric effects outside of the visible spectrum [10]. These large volumetric reference tables of meteorological data physically describe the impacts of clouds, precipitation, and aerosol haze for any spectral band and geometry within the cube. Figures 2- 4 depict a hypothetical volcanic plume for a 360 x 360 x 30 km volume centered over Lihue (Kauai Island), Hawaii at various spectral bands at 0000 UTC on 19 August 2016. Volcanic aerosols were placed at altitudes of 9 to 50 km with a peak in extinction near 30 km. In this case, clouds and rain used in the cube are determined from GFS output of vertical velocity and relative humidity (i.e., WWMCA is not used here). Total single scattering albedo is defined as the total scattering divided by total extinction, and a transparency scheme based on transmission values was applied to the images. High transmission values correlate to a transparent atmosphere, depicted as white. The opposite is true of low of low transmission values [10].

Copyright © 2017 Advanced Maui Optical and Space Surveillance Technologies Conference (AMOS) – www.amostech.com

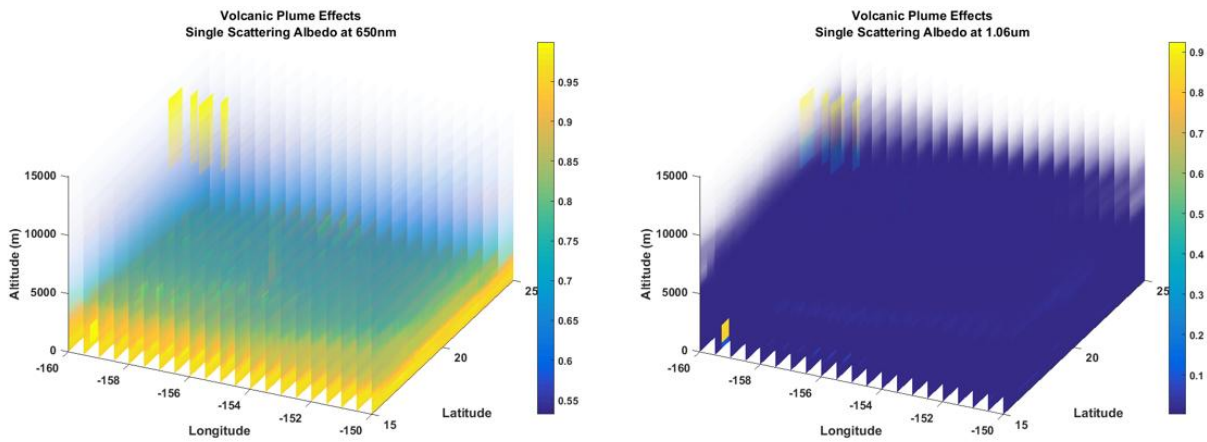

Fig. 2. Left: Single Scattering Albedo at 650nm. Right: Single Scattering Albedo at 1.06µm [10].

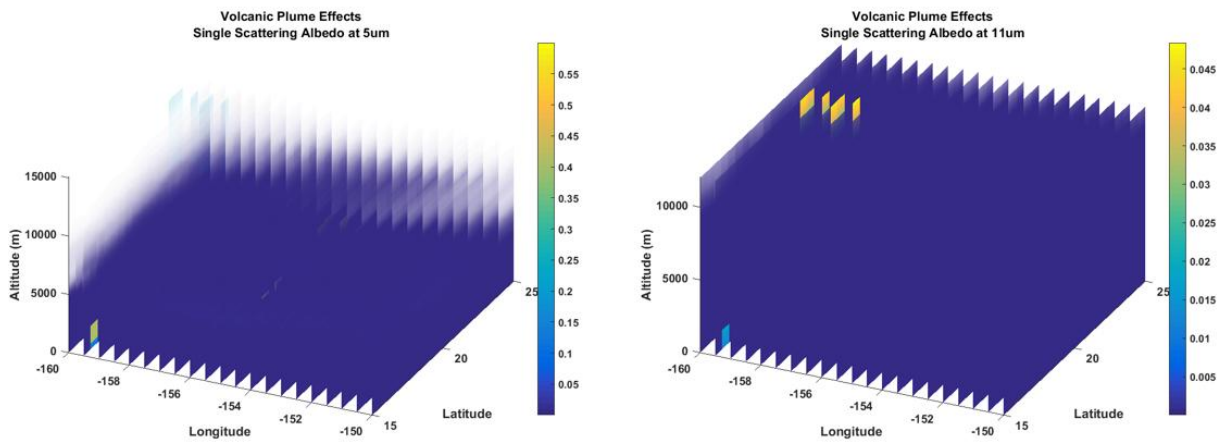

Fig. 3. Left: Single Scattering Albedo at 5.0µm. Right: Single Scattering Albedo at 11.0µm
(Note that volcanic plume values are enhanced with a factor of 10000 and that this affects the color scale) [10].

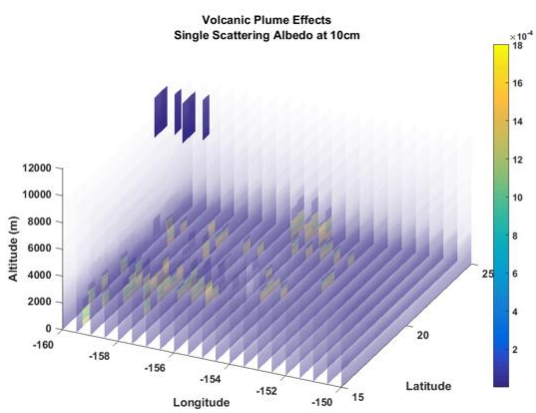

Fig. 4. Single Scattering Albedo at 10cm [10].

While weather cubes describe the atmospheric state and radiative transfer properties for a volumetric region, the effects through these geographic areas are of primary concern to operational users. Weather cubes can be leveraged to determine cloud effects of diffuse transmission, such as that from a modeled NUDET.

4. Results

Copyright © 2017 Advanced Maui Optical and Space Surveillance Technologies Conference (AMOS) – www.amostech.com

For this analysis, diffuse transmission is calculated by assuming a diffuse lambertian source as a model for NUDETS. Atmospheric profiles are built for each line of sight under investigation in the weather cube. A 1976 US Standard atmosphere was used for altitudes above 30,000 m, and a GFS defined atmosphere with WWMCA derived clouds was used for altitudes below 30,000 m. Utilizing the Discrete Ordinate Radiative Transfer Code (DISORT) [11], a sixteen stream multiple scattering calculation is employed to determine diffuse radiance at the sensor [4]. Diffuse transmission is evaluated for the 300-1300 nm band with a nominal sensor response function.

One of the primary objectives with NUDET detection is geolocation of source signals. If a source signal is known from non-imaging sensors, then it may be possible to use the atmosphere as a natural filter. To do so, the amount of attenuation for the detected signal must be known or estimated via modeling, comparison, or other means. By modeling source to sensor diffuse transmission for each potential line of sight, a map of diffuse transmission values can be generated and compared to known source characteristics. Consider the case of 2 January 2015. Figure 5 depicts the geographical cloud distribution at 0000 UTC.

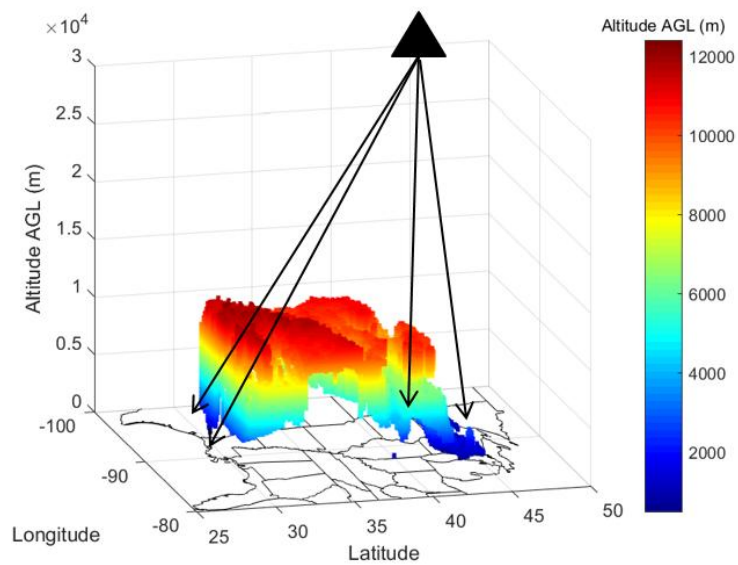

Fig. 5. Three dimensional representation of cloud conditions for 2 January 2015 at 0000 UTC. Shown are notional (not to scale) representations of source to satellite lines of sight [4].

It is important to note that Figure 5 only indicates the presence of clouds within a particular grid cell. The actual percentage of the grid cell area covered with clouds is not conveyed here, but is available in the WWMCA outputs. This analysis assumes that if any amount of clouds are present along the line of sight, they are encountered. In essence, this provides a worst case scenario. Statistical analysis utilizing the percentage of cloud cover would be useful for determining performance limitations.

Diffuse transmission for 2 January 2015 at 0000 UTC as seen by a sensor at 40.0º latitude, -90.0º longitude, and an altitude of 20,200 km is depicted in Figure 6. The four plots demonstrate the effects of using standard atmospheres and NWP for atmospheric characterization. Note that the large grid pattern evident in the lower plots results from using the 5 x 5 degree Global Aerosol Data Set (GADS, [12, 13, 14]), which is a worldwide database comprised of various aerosols species and concentrations specific to each region, and the subsequent aerosol effects. All results shown here include the GADS data. Locations without 100% cloud coverage often have some of the lowest diffuse transmission values (not shown). This is likely due to smaller scale weather systems not resolved at the 0.5 degree resolution of the GFS.

Copyright © 2017 Advanced Maui Optical and Space Surveillance Technologies Conference (AMOS) – www.amostech.com

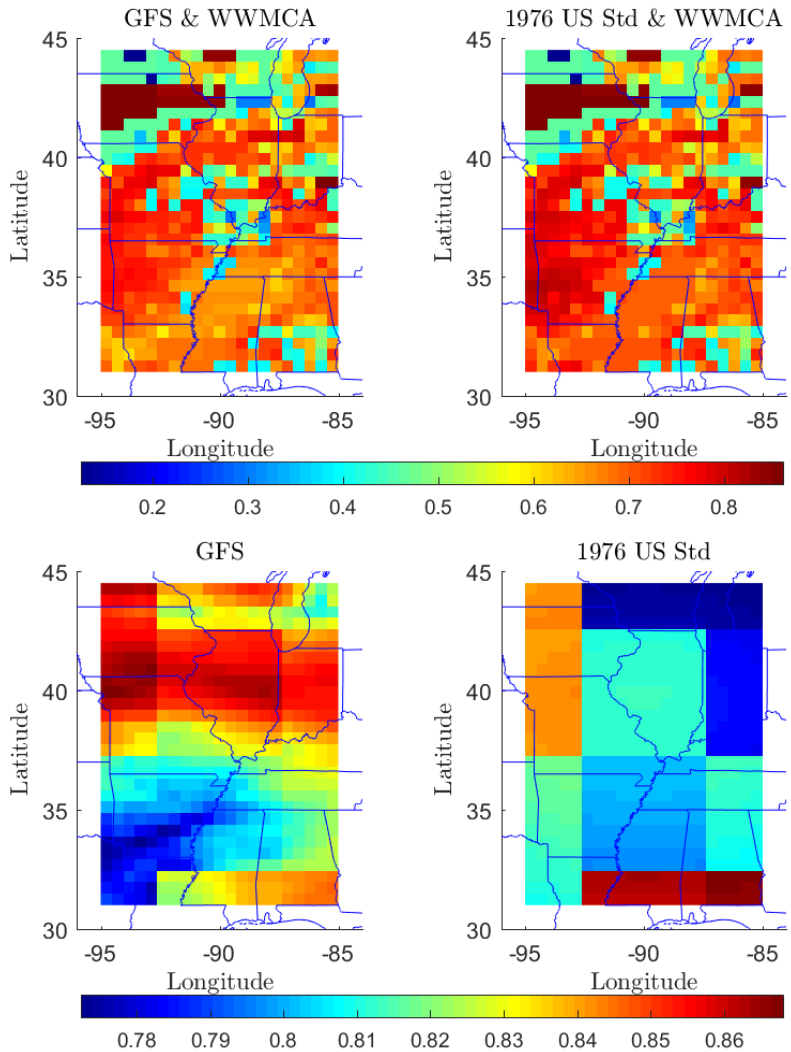

Fig. 6. Diffuse transmission for 2 January 2015 at 0000 UTC for a sensor located at 40.0º latitude, -90.0º longitude, and an altitude of 20,200 km for various atmospheric models. The upper left chart depicts the diffuse transmission when the GFS and WWMCA models are both utilized. The upper right models a standard atmosphere with WWMCA based clouds. The lower left models a cloud free atmosphere with GFS derived meteorological parameters while the lower right depicts a standard atmosphere without clouds [4].

Using a realistic atmosphere derived from NWP data has a sizeable impact when compared to standard atmospheres. In this particular case, including the NWP data has a potential ~8% (maximum) effect, reinforcing the importance of utilizing accurate NWP data, even in clouded conditions. While clouded conditions produce much more variability in absolute diffuse transmission results, the differences due to meteorological parameters (sans clouds themselves) is on the same scale as those observed in cloud free conditions [4].

We next examine the optical signal of lightning because it is often described as the natural phenomena that serves as a surrogate for a NUDET in terms of optical output. For this reason, comparisons are often made to lightning optical signatures. Spectrally, these two sources present themselves quite distinctly. Figure 7 shows a blackbody source and the effects of various atmospheric conditions on its propagation from source to a satellite sensor from the ground. It also depicts the same for lightning sources, adapted from the observations of Walker and Christian [15]. Both sources are normalized over the band such that the total integrated radiance is equal to one. The relative differences between the two were calculated for each of the 15,000 samples and several spectral lines/bands present themselves as potential discriminators. These tend to match traditional lightning detection bands for satellite based sensors. It is important to consider this type of analysis for any new detection system with spectral capability in order to maximize the detection of the source signature of interest.

Copyright © 2017 Advanced Maui Optical and Space Surveillance Technologies Conference (AMOS) – www.amostech.com

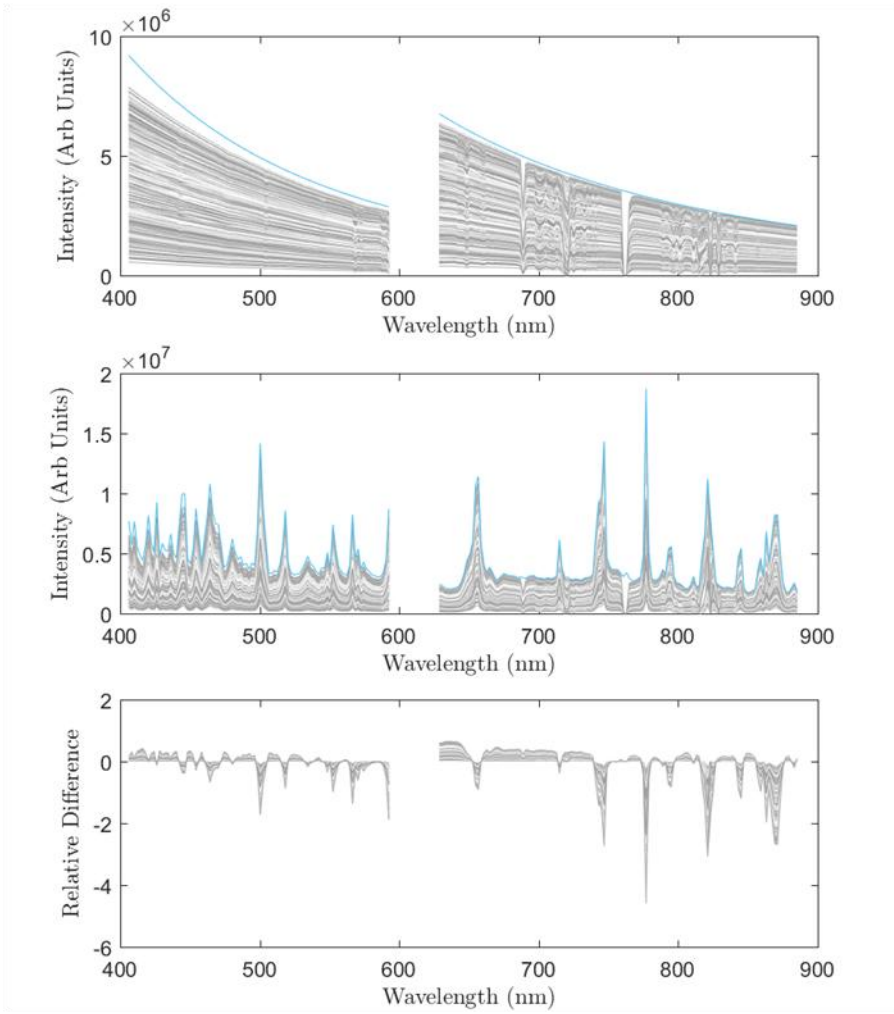

Fig.7. Top: 20,000 K blackbody diffuse transmission for various atmospheric conditions. Middle: Lightning diffuse transmission for various atmospheric conditions. Adapted from Walker and Christian [14]. For both plots the normalized source is shown in blue while the effects of 15,000 globally distributed atmospheric profiles are shown in gray. Bottom: Lightning and blackbody diffuse transmission relative differences for various atmospheric conditions. [4]

Another important aspect to consider is that diffuse transmission modeling for multiple lines of sight through a weather cube, such as would be required for an atmospheric filter over a large geographic region, can be computationally expensive. One way to lessen this burden is to find ways categorize the data before performing a calculation and only evaluate those pieces that are necessary. To this end, the combination of NWP and WWMCA data proves useful. For instance, the WWMCA data provides an opportunity to generate cloud free line of sight (CFLOS) probabilities. Figure 8 depicts the probability of CFLOS at four different times during the month of January as calculated from the 0000, 0600, 1200, and 1800 UTC 2015 data. Historically, CFLOS probabilities have been determined for nadir geometries from ground to space, without regard for azimuthal variation as they primarily supported aviation activities. Additionally, many of these products are generalized for regional climatological conditions, neglecting important effects due to local geography. By definition, a typical CFLOS product simply reports the presence of a cloud. Using a CFLOS model coupled with accurate cloud characterization provides the ability to assess impact or effect as opposed to only cloud presence. Here CFLOS is calculated between the various surface locations and a sensor located in geostationary orbit at 0º latitude, -75º longitude. Variations with time of day are evident as well as seasonal variation (not shown) [4].

Copyright © 2017 Advanced Maui Optical and Space Surveillance Technologies Conference (AMOS) – www.amostech.com

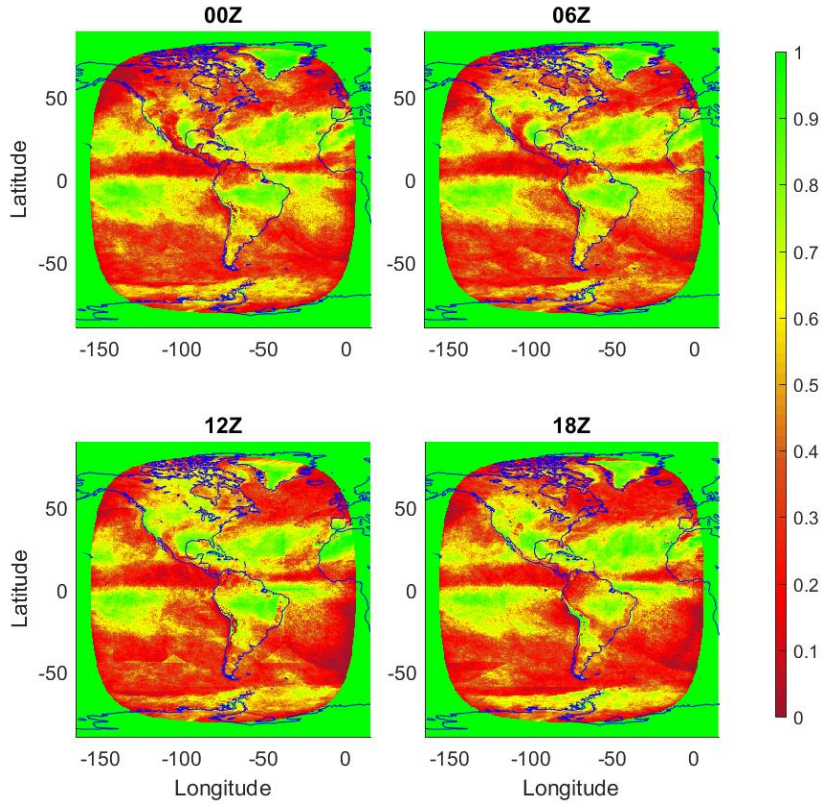

Fig. 8. CFLOS for ground locations when viewed by a sensor in geostationary orbit at 0º latitude, -75º longitude, for various times in January 2015. The circular region defines the area visible to the satellite while the green region on the exterior does not have a direct LOS [4].

Sorting based on CFLOS has the potential to reduce the number of simulations required to construct a useful atmospheric filter product for NUDET detection and geolocation. But, this does not decrease the expense for each computation still needed. One solution is to use a representative or proxy wavelength (or combination) to accurately describe the behavior of a sensor within a band. This is accomplished by selecting the optimal combination of wavelengths that best characterizes the band performance. By choosing only a few proxy wavelengths, the number of computations is greatly decreased, yet the band performance is confidently assessed. Fitting a linear-least-squares fit to the integrated band transmission as a function of a single (or multiple) wavelength(s) produces a fit that generates a band transmission given a single (or multiple) wavelength(s) diffuse transmission(s) as described by

$$t_b = at_{\lambda_1} + bt_{\lambda_2} + ct_{\lambda_3} ... + f,$$

where t_b is the band transmission, $t_{\lambda 1}$, $t_{\lambda 2}$, and $t_{\lambda 3}$ are the spectral transmission at selected wavelengths, and a - f are fitting coefficients. Fitting was accomplished for 500 evenly spaced wavelengths in the 300-1300 nm band, and the best fit was chosen from among the results. This iterative process was repeated, increasing the number of wavelength terms in the fit from one to five incrementally. The results were compiled for 15,000 different cases, all of which were nadir geometry at random dates/times/locations worldwide. Figure 9 summarizes the equations, confidence intervals, and errors associated with the proxy wavelength method described.

Copyright © 2017 Advanced Maui Optical and Space Surveillance Technologies Conference (AMOS) – www.amostech.com

Equation Parameters without Response Function					
Terms	1	2	3	4	5
a	9.82E-01	9.69E-01	7.59E-01	7.04E-01	5.51E-01
b		3.35E-02	5.60E-02	-8.35E-03	-3.92E-02
c			1.79E-01	2.20E-01	1.95E-01
d				6.01E-02	9.19E-02
e					1.81E-01
f	-1.18E-02	-6.96E-03	2.07E-02	2.87E-02	1.99E-02
λ (nm)	5.69E+02	1.14E+03	1.27E+03	1.16E+03	4.94E+02
Percentiles without Response Function					
Mean	-2.67E-06	4.32E-06	-4.45E-07	-3.11E-07	-5.26E-07
Median	-1.63E-03	-1.09E-03	-6.94E-04	7.82E-05	-2.59E-04
0.5^{th} Pctl	-1.93E-02	-1.77E-02	-1.13E-02	-1.10E-02	-7.17E-03
2.5^{th} Pctl	-1.48E-02	-1.31E-02	-8.51E-03	-8.54E-03	-5.70E-03
16th Pctl	-9.91E-03	-7.45E-03	-4.71E-03	-3.71E-03	-2.75E-03
84th Pctl	1.14E-02	7.72E-03	5.20E-03	3.22E-03	2.94E-03
97.5^{th} Pctl	2.09E-02	1.89E-02	1.09E-02	9.24E-03	6.43E-03
99.5^{th} Pctl	2.49E-02	2.45E-02	1.49E-02	1.39E-02	9.15E-03

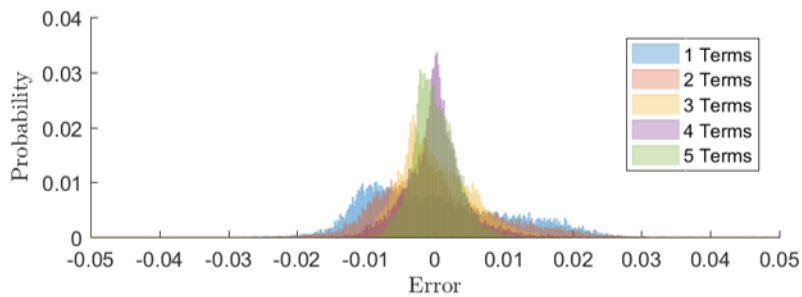

Fig. 9. Summary of confidence intervals, and errors associated with the proxy wavelength described in the text.

If a sensor response function were considered in this analysis, the proxy wavelengths would be distinctly different. Additionally, these results are specific to the source function (5,800 K blackbody) specified since band transmission is defined as the amount of energy transmitted across the band relative to the amount of source energy present in the band. Consequently, this type of analysis should be examined with respect anticipated sources and sensors. If multiple source functions are known, the processes could be utilized to develop parameterized scaling equations for each source and band [4].

5. Conclusions & Future Work

Optical sensing systems support a broad range of operational missions and research and development projects. These systems rely on optical signal sources and sensors that can each be located in any part of the Earth's and near-Earth environments and are separated by the atmosphere. Specifically, correctly accounting for real-time atmospheric clouds is essential, but has been hampered by the lack global real-time cloud models. For this research project, we are assimilating real-time cloud data into global models to assist in analysis of bright, impulsive optical sources (e.g., NUDETs, lightning) on the Earth's surface as seen by optical sensors on-orbit.

The broad objective of this research is to compute optical attenuation between two points located anywhere between the Earth's surface and near-Earth space. The specific objective is to include optical attenuation that accounts for local clouds in the optical ray path, specifically with the ability to compute an attenuation map to a single, non-imaging optical sensor for unknown but possible source locations in a defined geographic area. More explicitly, the individual objectives of this research are to:

1. Develop the capability to map clouds globally in real-time and high spatial resolution (weather cubes).

Copyright © 2017 Advanced Maui Optical and Space Surveillance Technologies Conference (AMOS) – www.amostech.com

2. Develop the capability to compute the ray paths through the correct weather cubes.
3. Compute the optical attenuation along that ray path, accounting for source spectra and sensor response.
4. Compute an attenuation map, as seen by a satellite sensor, for the sensor's entire field of view.
5. Match measured with computed attenuation maps to place bounds on geolocation solutions.

This paper demonstrates progress where:

1. Weather cubes for selected areas have been computed.
2. Computing ray paths through the weather cubes is in progress.
3. Computing the attenuation has been demonstrated, for specific cases.
4. An attenuation map has been demonstrated, but not yet mapped to the view of a satellite sensor.

Results thus far show that global cloud observations can be converted into arrays of cubes with sides that are approximately 25 km each. Combining global atmospheric meteorological and cloud conditions into a "weather cube" enables computation of optical attenuation for any ray path across the spectrum. When the sensor side of the ray path is at a fixed location (e.g., satellite), and the source end is at a known location on the Earth's surface, then comparing measured with modeled optical attenuations proves a means to validate a sensor measurement. In the case where the source location is unknown, the attenuation can be modeled for the entire area within the sensor's field of view and leveraged in comparisons to the sensor's measured optical attenuation, thus providing bounds on a geolocation solution set. Mapping this comparison will provide a means of bounding the source geolocation for analysis.

Future planning is to extend this capability to an automated process that will work in a near real-time operational environment and be tested for practical use.

The work in this paper and presentation is the result of close collaboration among the Atmosphere and Space Division, the Meteorological Modeling and Analysis Division, both at the Air Force Technical Applications Center, and the Air Force Institute of Technologies Center for Directed Energy.

6. REFERENCES

1. Shirey, S. M., 2016. "A Relative Humidity Based Comparison of Numerically Modeled Aerosol Extinction to LIDAR and Adiabatic Parameterizations." Air Force Institute of Technology, 65 pp.
2. National Oceanic and Atmospheric Administration, National Weather Service, National Centers for Environmental Prediction, Environmental Modeling Center. "The Global Forecast System (GFS) - Global Spectral Model (GSM)." [Online]. Available: http://www.emc.ncep.noaa.gov/GFS/doc.php
3. National Oceanic and Atmospheric Administration, National Weather Service, National Centers for Environmental Prediction, Environmental Modeling Center. "The Global Forecast System (GFS) - Global Spectral Model (GSM)." [Online]. Available: http://www.emc.ncep.noaa.gov/GFS/doc.php
4. Burley, J.L., 2017. "A Computational Tool for Hyperspectral Propagation of NUDET Effects." Air Force Institute of Technology, 200 pp. (Available through request to the Air Force Institute of Technology).
5. AFWA/2WXG/16WS. "Algorithm Description Documentation for the Cloud Depiction and Forecast System II," p. 516, Air Force Weather, 2nd Weather Group, OFFUTT AFB, Nebraska (2 July 2013). (Available through request to the USAF 557th Weather Wing).
6. Arduini, R. F., et al. "Sensitivity of satellite-retrieved cloud properties to the effective variance of cloud droplet size distribution." Proc. 15th ARM Science Team Meeting. 2005.
7. Wiscombe, W.J., "Improved Mie scattering algorithms," *Appl. Opt.* 19, 1505-1509 (1980).
8. Hall, D., J. Madry, and D. Courtney, 2016: Verification and Validation Report for High Energy Laser (HEL) Joint Technical Office (JTO) Laser Environmental Effects Definition & Reference (LEEDR) Version 4.0 Patch 17. NAVAIR Simulation Division Verification and Validation Rep. (Available through request to the Air Force Institute of Technology).
9. Fiorino, S.T., R. M. Randall, M. F. Via, and J. L. Burley, 2014: Validation of a UV-to-RF high-spectral-resolution atmospheric boundary layer characterization tool. *J. Appl. Meteol. Climatol.*, **53**, 136–156.
10. Schmidt, J., Fiorino, S., Burley, J., Elmore, B. "*Multi-spectral Weather Cubes for atmospheric plume*

Copyright © 2017 Advanced Maui Optical and Space Surveillance Technologies Conference (AMOS) – www.amostech.com

characterization," in Imaging and Applied Optics 2017, OSA Technical Digest (online) (Optical Society of America, 2017).
11. Stamnes, K., SC. Tsay, W. Wiscombe and K. Jayaweera, 1988: Numerically stable algorithm for discrete-ordinate-method radiative transfer in multiple scattering and emitting layered media. *Appl. Optics*, **27**, 12, 2502-2509.
12. d'Almeida, G.A., P. Koepke, and E.P. Shettle, 1991: *Atmospheric Aerosols: Global Climatology and Radiative Characteristics*. A. Deepak Publishing, 561 pp.
13. Hess, M., P. Koepke, and I. Schult, 1998. "Optical properties of aerosols and clouds: The software package OPAC." *Bull. Am. Meteorol. Soc.*, **79**, 831–844.
14. Koepke, P., M. Hess, I. Schult, and E. P. Shettle, 1997: Global aerosol data set. *MPI Meteorol. Hambg. Rep* 243, 44 pp. [Available online at [https://www.mpimet.mpg.de/fileadmin/publikationen/Reports/MPI-Report_243.pdf.]
15. Walker, T.D. and H. J. Christian, "Novel observations in lightning spectroscopy," in *XV International Conference on Atmospheric Electricity, Norman, Oklahoma*, 2014.

Copyright © 2017 Advanced Maui Optical and Space Surveillance Technologies Conference (AMOS) – www.amostech.com